

FPrev: Revealing the Order of Floating-Point Summation by Numerical Testing

PEICHEN XIE, YANJIE GAO, and JILONG XUE, Microsoft Research

The order of floating-point summation is a key factor in numerical reproducibility. However, this critical information is generally unspecified and unknown for most summation-based functions in numerical libraries, making it challenging to migrate them to new environments reproducibly. This paper presents novel, non-intrusive, testing-based algorithms that can reveal the order of floating-point summation by treating functions as callable black boxes. By constructing well-designed input that can cause the swamping phenomenon of floating-point addition, we can infer the order of summation from the output. We introduce FPrev, a tool that implements these algorithms, and validate its efficiency through extensive experiments with popular numerical libraries on various CPUs and GPUs (including those with Tensor Cores). FPrev reveals the varying summation orders across different libraries and devices, and outperforms other methods in terms of time complexity. The source code of FPrev is at <https://github.com/microsoft/RepDL/tree/main/tools/FPrev>.

1 INTRODUCTION

With the rapid evolution of heterogeneous hardware and diverse software stacks, the lack of reproducibility in numerical computing has become a recognized problem [2, 4, 13, 21, 29, 30]. The same numeric function can produce varying results when software is migrated to new hardware or when numerical libraries are updated. Non-reproducible results pose significant challenges in scientific research, software engineering, deep learning, and applications that rely on numerical models for decision making. These challenges undermine the credibility of findings, hinder progress by obscuring errors in programs, and can lead to incorrect conclusions or suboptimal decisions, ultimately affecting the reliability and trustworthiness.

A primary cause of numerical non-reproducibility is discrepancies in the order of floating-point summation [1, 6, 8, 9, 27]. The result of floating-point summation depends on the order of computation due to the non-associative nature of floating-point addition. For example, as shown in Table 1, the sum of 0.1, 0.2 and 0.3 is order-dependent, because $(0.1 + 0.2) + 0.3 \neq 0.1 + (0.2 + 0.3)$ in IEEE-754 [16] binary64 (also known as float64). There is no general specification that stipulates the order of floating-point summation. Consequently, without well-defined specifications, numerical libraries usually compute floating-point summation in various orders in different environments, leading to inconsistent numerical output.

Table 1. Examples of the non-associative nature of float64 addition.

	$(0.1 + 0.2) + 0.3$	$0.1 + (0.2 + 0.3)$	$(-2^{60} + 2^{60}) + 1$	$-2^{60} + (2^{60} + 1)$
Decimal	0.60000000000000008882	0.5999999999999997780	1	0
Hexadecimal	0x1.3333333333334p-1	0x1.3333333333333p-1	0x1p0	0x0p0

Knowing the order of summation is critical for reproducibility. Consider a function based on floating-point summation (e.g., matrix multiplication) that produces inconsistent output in new environments, which is undesirable. To fix the issue, the order of summation must be known. This information can serve as a valuable guide and constraint in determining the appropriate order of summation when migrating the function to the new environments. However, the information is virtually unknown. Existing numerical libraries, such as Intel MKL [17], OpenBLAS [7], and NVIDIA cuBLAS [24], do not specify this information in their documentation, and there is no specialized tool to reveal the information.

Revealing the order of summation is a challenging task. For example, people can manually determine the order by analyzing the static source code, but many libraries or hardware implementations are black-box, which limits the static approach. Even if the function’s trace is obtained and analyzed, no tool can automatically generate the computational graph of the summation.

We build a non-intrusive, testing-based tool called FPRev to reveal the order of summation. FPRev treats the summation-based function as a callable black box, generates specialized test cases, and infers the order of summation from the function’s output. FPRev provides two versions of algorithms: FPRev-basic and FPRev-advanced. Both leverage the swamping phenomenon in floating-point addition to generate well-designed numerical input. When two floating-point numbers differing by many orders of magnitude are added, the smaller number is swamped and does not contribute to the sum. For example, $2^{60} + 1$ equals 2^{60} when using float64. Based on the phenomenon, we can utilize large numbers as masks to hide certain summands from the sum.

In FPRev-basic, we first generate several “masked all-one arrays”. Each array is predominantly composed of the floating-point number 1.0, with exactly two non-one elements: M and $-M$. Here, M represents a large positive number that can cause the swamping phenomenon in floating-point arithmetic. Specifically, let n denote the number of summands. M satisfies $\pm M + \mu = \pm M$ for all non-negative number $\mu < n$.

Next, we call the tested function multiple times with different masked all-one arrays. Each output reveals how many summands are swamped by $\pm M$ during summation and how many are not. This information relates to the structure of the computational graph. The graph is a full binary tree that accurately depicts the order of operations. Each output equals the number of leaf nodes out of the subtree rooted at the lowest common ancestor of the nodes corresponding to the indexes of M and $-M$. For example, Table 2 demonstrate the information for Algorithm 1, whose computational graph is Figure 1.

Finally, we use the output information to construct the summation tree. This involves a tree-algorithm problem: how to construct a full binary tree given $\{(i, j, l^{i,j}) : 0 \leq i < j < n\}$, where $l^{i,j}$ denotes how many leaf nodes are in the subtree rooted at the lowest common ancestor of the i -th and j -th leaf nodes. We construct the tree in a bottom-up (leaf-to-root) way. We begin by constructing subtrees with two leaf nodes (corresponding to $l^{i,j} = 2$). Subsequently, larger subtrees (corresponding to next larger $l^{i,j}$) are built from existing subtrees or isolate nodes, and the process is repeated until the entire tree is generated.

Algorithm 1 An example of summation ($n = 8$).

```
float sum = 0;
for (int i=0; i<8; i+=2)
    sum += a[i] + a[i+1];
```

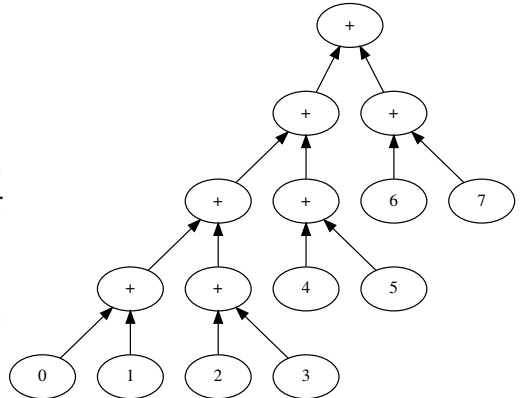


Fig. 1. The summation tree of Algorithm 1. The numbers in the leaf nodes denote the indexes.

Table 2. The outputs and order-related information for Algorithm 1 with different masked all-one arrays.

i	j	$A^{i,j}$	$\text{SUM}(A^{i,j})$	$l^{i,j}$
0	1	$(M, -M, 1, 1, 1, 1, 1)$	6	2
0	2	$(M, 1, -M, 1, 1, 1, 1)$	4	4
0	3	$(M, 1, 1, -M, 1, 1, 1)$	4	4
0	4	$(M, 1, 1, 1, -M, 1, 1)$	2	6
0	5	$(M, 1, 1, 1, 1, -M, 1)$	2	6
0	6	$(M, 1, 1, 1, 1, 1, -M)$	0	8
0	7	$(M, 1, 1, 1, 1, 1, -M)$	0	8
		...		
2	3	$(1, 1, M, -M, 1, 1, 1)$	6	2
2	4	$(1, 1, M, 1, -M, 1, 1)$	2	6
		...		

FPrev-basic has a time complexity of $\Theta(n^2t(n))$, where $t(n)$ is the time complexity of the tested function. As a contrast, the naive brute-force method has a time complexity of $O(4^n/n^{3/2} \cdot t(n))$. Building on FPrev-basic, we propose FPrev-advanced, which has a time complexity of $\Omega(nt(n))$ and $O(n^2t(n))$ and supports multi-term fused summation [10] used by matrix accelerators like NVIDIA GPU’s Tensor Cores [22].

We evaluate efficiency of FPrev by comprehensive experiments. We test FPrev with three popular numerical libraries across six different CPUs and GPUs. Experimental results show that FPrev-advanced is significantly faster than FPrev-basic, demonstrating its lower time complexity. We also showcase the discrepancies in the revealed orders across different libraries and devices.

In summary, the contributions of this paper include the following:

- (1) We propose novel testing-based algorithms to reveal the order of summation for functions based on floating-point summation. The time complexity of the algorithms is polynomial, in contrast to the exponential time complexity of the naive approach.
- (2) We develop FPrev, a tool that enables automatic revelation of the order of floating-point summation. This tool is significantly helpful in debugging non-reproducible programs, and provides useful information for reproducing the program.
- (3) We demonstrate the practical efficiency of FPrev with extensive experiments.
- (4) We reveal the order of summation for common numerical libraries like cuBLAS for the first time.

2 PROBLEM STATEMENT

2.1 Definition of the problem

We formulate the ordinary summation algorithm in Algorithm 2. To calculate the sum of n floating-point numbers, the floating-point addition is performed $n - 1$ times in a predetermined order. We assume that the order of summation is unknown but unique to the given function, computational environment, and n (the number of floating-point numbers in the input).¹

The order of summation can be represented as a computational graph in the form of a rooted full binary tree with n leaf nodes and $n - 1$ inner nodes. Each addition operation corresponds to an inner node, which represents the sum. The two children of the node represent the two summands of

¹Therefore, randomized algorithms and algorithms where the order depends on the values of the summands are out of scope.

Algorithm 2 The ordinary summation algorithm.

Require: Sequence $A = (a_0, a_1, \dots, a_{n-1})$

Ensure: Floating-point sum $\sum_{k=0}^{n-1} a_k$

```
function SUM( $A$ )
   $A \leftarrow$  MultiSet( $A$ )
  for  $k \leftarrow 0$  to  $n - 1$  do
    Choose  $a \in A$  and  $b \in A - \{a\}$  deterministically
     $c \leftarrow$  fl( $a + b$ ) ▷ floating-point addition
     $A \leftarrow A - \{a, b\} + \{c\}$ 
  return  $c$  ▷ now  $A = \{c\}$ 
```

this addition operation. For example, consider the program shown in Algorithm 1. The summation tree shown in Figure 1 depicts the order of summation of the program.

The problem is how to reveal the order of summation for a black-box summation function `SUM`. Specifically, we aim to design an algorithm whose input is the summation function (as a callback), and the number of summands n . The output of the algorithm is the summation tree.

2.2 Inefficiency of the naive solution

Here we introduce a naive testing-based solution to the problem. The naive solution is based on brute-force search. We design a recursive function to enumerate the order of summation, as shown in Algorithm 3. For each order, we verify its correctness by random testing. Specifically, in `VERIFY`, we generate random input, compute the sum in that order, and compare the output with the output of the summation function. If they are identical for ν trials, we accept the order.

Algorithm 3 The brute-force algorithm.

Require: Summation function `SUM`, number of summands n , and number of trials ν

Ensure: Summation tree T

```
function BRUTEFORCE( $SUM, n, \nu$ )
  function VERIFY( $T$ )
    for  $\nu$  times do
       $A \leftarrow$  Random( $n$ ) ▷ random array of size  $n$ 
       $s \leftarrow$  SUM( $A$ )
       $t \leftarrow$  ComputeSum( $A, \text{order} = T$ )
      if  $s \neq t$  then
        return False
    return True
  for each possible summation tree  $T$  do
    if VERIFY( $T$ ) then
      return  $T$ 
```

The time complexity of the naive solution is $O(4^n/n^{3/2} \cdot t(n))$, because the number of all possible orders is the $(n - 1)$ -th Catalan number $C_{n-1} = \frac{(2n-2)!}{n!(n-1)!} = O(4^n/n^{3/2})$. Here, $t(n)$ is the time complexity of the tested function. In addition to being inefficient, the naive solution is not fully reliable, because different orders can lead to the same output for some input. Although the probability is low and the reliability can be improved by increasing ν , a deterministic solution with full reliability is preferable.

2.3 Extension of the problem

We also wish to reveal the order of summation for functions that can be abstracted as calls to the summation function with intermediate results as input. We call them “summation-based functions”. For example, dot product $\mathbf{x} \cdot \mathbf{y}$ can be treated as $\text{SUM}((x_0y_0, x_1y_1, \dots, x_{n-1}y_{n-1}))$. Thus, solutions to the original problem can be naturally extended to the problem for summation-based functions.

3 FPREV-BASIC

This section demonstrates the basic algorithm FPRev-basic of our testing-based tool FPRev for revealing the order of floating-point summation. FPRev-basic has three stages.

3.1 Constructing masked all-one arrays

The first stage is to construct different “masked all-one arrays”, which are explained below. Let n be the number of summands, and let SUM be an implementation of Algorithm 2 with a predetermined but unknown order of summation. Let M be a floating-point number with the largest exponent, for example, $M = 2^{127}$ for float32 or $M = 2^{1023}$ for float64. We then define a masked all-one array superscript i, j as $A^{i,j} = (a_0^{i,j}, a_1^{i,j}, \dots, a_{n-1}^{i,j})$ such that

$$a_k^{i,j} = \begin{cases} M & \text{if } k = i \\ -M & \text{if } k = j \\ 1.0 & \text{otherwise} \end{cases}$$

where i and j denote the indexes of M and $-M$, respectively. In $A^{i,j}$, there exist exactly one M and one $-M$, with all other elements being 1.0.

In $\text{SUM}(A^{i,j})$, adding any summand or intermediate sum (except M and $-M$ themselves) to $\pm M$ results in $\pm M$. Specifically, $M + \mu = M$ and $-M + \mu = -M$ hold for $0 \leq \mu \leq n - 2$ in floating-point arithmetic, if $n \ll M$. This demonstrates the swamping phenomenon of floating-point addition [15]. Therefore, M and $-M$ serve as masks, swamping the summands or intermediate sums added to them.

As a result, the sum of a masked all-one array $A^{i,j}$ depends on the order of summation. For example, given $n = 4$ and $A^{0,2} = (M, 1, -M, 1)$, the resulting sum can be 0, 1, or 2, depending on the order of summation. Pairwise summation $(M + 1) + (-M + 1)$ yields 0, sequential summation $M + 1 + (-M) + 1$ yields 1, and stride summation $M + (-M) + (1 + 1)$ yields 2.

In this stage, we construct different masked all-one arrays by enumerating the locations of the masks, i.e., i and j . There are $n(n - 1)/2$ different arrays, which are $\{A^{i,j} : 0 \leq i < j < n\}$.

3.2 Inferring order-related information

The second stage is to identify the order-related information from the numerical output obtained using the constructed arrays as the input. The purpose of constructing masked all-one arrays is to leverage the masks to reveal information related to the order of summation. Because the masks swamp the summands or intermediate sums added to them, these numbers have no contribution to the sum. As a result, these summands are hidden by the masks. In contrast, only those summands not hidden by the masks contribute to the sum.

Therefore, the output equals the sum of the summands that are not hidden by the masks. Since each of the summands equals 1.0, the output equals the number of the summands not hidden by the masks:

$$n_{\text{unhidden}}^{i,j} = \text{SUM}(A^{i,j}).$$

Then, we can also obtain the number of the summands hidden by the masks:

$$n_{\text{hidden}}^{i,j} = n - 2 - n_{\text{unhidden}}^{i,j}.$$

Take Algorithm 1 as an example. If $i = 2$ and $j = 4$, then the array $A^{2,4}$ is $(1, 1, M, 1, -M, 1, 1, 1)$. Computing the sum in the order shown in Figure 1, the 3rd summand and the intermediate sum of the 0th and 1st summands are swamped by M , so the 0th, 1st and 3rd summands are hidden by M ; the 5th summand is swamped by $-M$, so in total, $n_{\text{hidden}}^{2,4} = 4$. In contrast, the 6th and 7th summands and their intermediate sum are not added to M or $-M$, so $\text{SUM}(A^{2,4}) = n_{\text{unhidden}}^{2,4} = 2$.

How does this information relate to the order, or specifically, the summation tree? Recall that i and j denote the locations of the masks, represented by the i -th and j -th leaf nodes in the summation tree. **We note that the neutralization of the two masks (i.e., the addition operation $M + (-M) = 0$) is represented by the lowest common ancestor of the i -th and j -th leaf nodes.** Then, observing the subtree rooted at the lowest common ancestor, we find that all the summands hidden by the masks are in the subtree, and all the summands not hidden by the masks are out of the subtree. Therefore, the size of the subtree, defined as the number of leaf nodes in the subtree, equals $n - n_{\text{unhidden}}^{i,j}$. Then we have

$$n_{\text{leaves}}^{\text{LCA}(i,j)} = n - n_{\text{unhidden}}^{i,j} = n - \text{SUM}(A^{i,j}).$$

For simplicity, we use $l^{i,j}$ to denote $n_{\text{leaves}}^{\text{LCA}(i,j)}$, "the number of leaf nodes in the subtree rooted at the lowest common ancestor of the i -th and j -th leaf nodes", in the rest of the paper.

In the previous example where $i = 2$ and $j = 4$, the lowest common ancestor of the 2nd and 4th leaf nodes is the parent node of the 4th leaf node, corresponding to the neutralization of the 2nd summand M and the 4th summand $-M$. Within the subtree rooted there, there are the 0th, 1st, 2nd, 3rd, 4th, and 5th leaf nodes, corresponding to the two masks and the summands hidden by the masks. In contrast, the 6th and 7th leaf nodes, corresponding to the unhidden summands, are out of the subtree. Therefore, $l^{2,4} = n_{\text{leaves}}^{\text{LCA}(2,4)} = 8 - 2 = 6$. Table 2 shows more examples of the summation results and the order-related information for Algorithm 1.

In summary, in this stage, we call the function with different masked all-one arrays, obtain the output of $\text{SUM}(A^{i,j})$, and infer the order-related information $L = \{(l^{i,j}, i, j)\}$ from the output by calculating

$$l^{i,j} = n - \text{SUM}(A^{i,j}). \quad (1)$$

3.3 Generating the summation tree

The third stage is to generate the summation tree from the order-related information obtained. Now, generating the tree from L is an algorithmic problem about trees.

The basic idea of our solution is to construct the tree using a bottom-up approach. We first sort L in ascending order. Then, according to each $l^{i,j}$, we find the existing roots of the trees containing the i -th and j -th leaf nodes respectively, and merge them by constructing a new parent node for them. Repeating this process, we generate the tree from small subtrees to large subtrees.

For example, consider the order-related information shown in Table 2. To generate the summation tree, we start by initializing the tree with eight disjoint nodes labeled 0 to 7. Then, examining the smallest value in L , we have $l^{0,1} = 2$. This signifies that the 0th and 1st leaf nodes should be in a subtree with 2 leaf nodes. Since the summation tree is a full binary tree, the 0th and 1st leaf nodes are exactly the two children of the root of the subtree. Therefore, we add a new node to the tree, label it with n plus the label of its left child (i.e., $n + 0$ in this example), and add two edges from the two leaf nodes to the new node.

For $l^{2,3} = l^{4,5} = l^{6,7} = 2$, similarly, we can construct the subtrees with the 2nd and 3rd, 4th and 5th, and 6th and 7th leaf nodes as their leaf nodes. Then, we have four subtrees of size 2, where the size of a subtree is defined as the number of leaf nodes in it.

Next, the smallest unexamined value in L is $l^{0,2} = 4$. This signifies that the 0th and 2nd leaf nodes should be in a subtree with 4 leaf nodes. We note that the 0th and 2nd leaf nodes are currently in two subtrees of size 2, so we should merge the two subtrees. Therefore, we find the current roots of the trees containing the 0th and 2nd leaf nodes respectively, denoted by $i' = n + 0$ and $j' = n + 2$. Then, we add a new node as the parent of i' and j' , label it with n plus the label of its left child (i.e., $n + i' = 2n + 0$ in this example), and add two edges from i' and j' to the new node.

For $l^{0,3} = 4$, we find that the 0th and 3rd leaf nodes are already in the same subtree of size 4, so we just skip it. The same process is applied to $l^{1,2} = l^{1,3} = 4$. Then, we have a subtree of size 4 and two subtrees of size 2.

The next smallest unexamined value in L is $l^{0,4} = 6$, which signifies that the 0th and 4th leaf nodes should be in a subtree with 6 leaf nodes. Similarly, the 0th and 4th leaf nodes are currently in two subtrees of size 4 and 2, respectively, so we should merge the two subtrees. Therefore, following the similar process, we find the current roots of the trees containing the 0th and 4th leaf nodes respectively (i.e., $i' = 2n + 0$, $j' = n + 4$). Then, we construct a new node as their parent (labelled as $n + i' = 3n + 0$), and add two edges from i' and j' to it.

For $l^{0,5} = 6$, we find that the 0th and 5th leaf nodes are already in the same subtree of size 6, so we skip it. The same process is applied to $i \in \{1, 2, 3\}$ and $j \in \{4, 5\}$. Then, we have a subtree of size 6 and a subtree of size 2.

Finally, in the similar way, the next smallest unexamined value in L is $l^{0,6} = 8$, which signifies that the 0th and 6th leaf nodes should be in a subtree with 8 leaf nodes. Since the two leaf nodes are currently in two subtrees of sizes 6 and 2, respectively, we should merge the two subtrees accordingly. After we add the parent node of the current roots of the two subtrees and add the corresponding edges, the entire summation tree is generated.

To generalize and formulate the algorithm, we present Algorithm 4, which combines the three stages. The GENERATETREE part encapsulates the third stage. For each $l^{i,j}$, we find the existing roots of the trees containing the i -th and j -th leaf nodes, denoted by i' and j' . If they are identical, then the i -th and j -th leaf nodes are already in the same subtree. Otherwise, we combine them. The FindRoot function can be implemented by the disjoint-set data structure, resulting in an amortized time complexity of $O(\alpha(n))$ [28], where $\alpha(n)$ is the inverse Ackermann function.

3.4 Time complexity and correctness

The time complexity of the input construction is $\Theta(n^2)$. Let $t(n)$ be the time complexity of SUM, the computation of L has a time complexity of $\Theta(n^2 t(n))$. In the tree generation stage, the time complexity of sorting $n(n - 1)/2$ elements is $\Theta(n^2 \log n^2) = \Theta(n^2 \log n)$. Therefore, the time complexity of tree generation stage is $\Theta(n^2 \log n + n^2 \alpha(n)) = \Theta(n^2 \log n)$. Thus, the overall time complexity of FPRev-basic is $\Theta(n^2) + \Theta(n^2 t(n)) + \Theta(n^2 \log n) = \Theta(n^2 t(n))$.

The correctness of FPRev-basic is guaranteed by design and can be proved as follows. For a given function SUM and n , we use T to denote the real summation tree and define $T' = \text{FPREVBASIC}(\text{SUM}, n)$. Assuming $T \neq T'$, there must exist i and j such that $l_T^{i,j} \neq l_{T'}^{i,j}$. Now we construct $A^{i,j}$ and compute its sum in the order T and T' respectively, resulting in s and s' . Then, $s = n - l_T^{i,j} \neq s' = n - l_{T'}^{i,j}$. However, since $s = \text{SUM}(A^{i,j})$, then $l_{T'}^{i,j} = n - s' \neq n - s = n - \text{SUM}(A^{i,j})$. This contradicts the statement $l^{i,j} \leftarrow n - \text{SUM}(A^{i,j})$ in Algorithm 4. Therefore, the assumption $T \neq T'$ is false, so $T = T'$.

Algorithm 4 FPRev-basic.

Require: Summation function SUM and number of summands n

Ensure: Summation tree T

function FPREVBASIC(SUM, n)

$L \leftarrow \emptyset$

for $i \leftarrow 0$ to $n - 1$ **do**

for $j \leftarrow i + 1$ to $n - 1$ **do**

 Construct $A^{i,j}$

$l^{i,j} \leftarrow n - \text{SUM}(A^{i,j})$

$L \leftarrow L \cup \{(l^{i,j}, i, j)\}$

function GENERATETREE(L)

$T \leftarrow \emptyset$

for $(l^{i,j}, i, j) \in L$ in ascending order **do**

$i' \leftarrow T.\text{FindRoot}(i)$

$j' \leftarrow T.\text{FindRoot}(j)$

if $i' \neq j'$ **then**

$k \leftarrow i' + n$

 ▶ assign a new label

$T \leftarrow T \cup \{(i', k), (j', k)\}$

return T

return GENERATETREE(L)

4 FPREV-ADVANCED

This section demonstrates the advanced algorithm FPRev-advanced of our tool FPRev. We first modify FPRev-basic for optimized efficiency. Then, based on the optimized version, we add support for multi-term fused summation used by matrix accelerators like NVIDIA GPU's Tensor Cores.

4.1 Optimization

4.1.1 Recursive process. Observing FPRev-basic, we note that Algorithm 4 requires $n(n - 1)/2$ elements of L as input, and many values of $l^{i,j}$ are the same. However, only $n - 1$ new nodes and $2(n - 1)$ new edges are constructed. Since obtaining multiple $l^{i,j}$ by calling SUM constitutes the primary cost of the method, reducing redundancy in $l^{i,j}$ (i.e., the cases $i' = j'$ in Algorithm 4) can significantly improve efficiency.

To achieve this, we will calculate $l^{i,j}$ on demand. Specifically, we do not calculate all $l^{i,j}$ ahead of the tree generation stage. Instead, we directly enter the tree generation stage, and calculate $l^{i,j}$ when needed. Following the bottom-up idea, we still construct subtrees from leaf to root.

First step. We use the set $I = \{0, 1, \dots, n - 1\}$ to denote the indexes of the leaf nodes. Let i represent the leaf node with the smallest index in I . The sibling node of i is either a leaf node or an inner node. If it is a leaf node, there must be a unique j such that $l^{i,j} = 2$. Otherwise, if it is an inner node, then $l^{i,j} > 2$ for all j such that $j \neq i$. Therefore, to distinguish the two cases, we need to calculate $l^{i,j}$ for all other leaf nodes, denoted by the set $L_i = \{l^{i,j} : j \in I - \{i\}\}$. We examine the minimum value in L_i , which is denoted by $l = \min(L_i)$.

If l equals 2, let j be the one that satisfies $l^{i,j} = 2$. Then, the j -th leaf node is the sibling node of i , so we add a new node to the tree, and add two edges from the i -th and j -th leaf node to the new node. The size of the currently constructed subtree is 2 now.

Otherwise, if l is larger than 2, the sibling node of i must be an inner node. The subtree rooted at this inner node must have $l - 1$ leaf nodes. Let $J_l = \{j : j \in I - \{i\} \wedge l^{i,j} = l\}$. Then, the number of

members of J_l must be $l - 1$, and the members of J_j must be the leaf nodes of this subtree. This can be proved by contradiction. Now, constructing this subtree is a subproblem for the leaf nodes J_j . Suppose that we have constructed this subtree by a recursive algorithm. We shall add a new node to the tree, and add edges from i and the root node of this subtree to the new node. Now, the size of the currently constructed subtree is l .

Summarizing the two cases, we can treat both cases as the same recursion process: finding $J_l = \{j : j \in I - \{i\} \wedge l^{i,j} = l\}$ and solving the subproblem for J_l . The first case (where $|J_l| = 1$) just leads to the stop condition of the recursion (where $|I| = 1$).

Second step. Now we have constructed a subtree of size l . Let r be the root of this subtree. Similarly, to find the sibling node of r , we examine the minimum value in the rest of L_i , which is denoted by l' here. Then, we solve the subproblem for $J_{l'} = \{j : j \in I - \{i\} \wedge l^{i,j} = l'\}$, and get a subtree with leaf nodes $J_{l'}$. The root of the subtree, whether a leaf node or an inner node, is the sibling node of r . Therefore, we shall add a new node to the tree, and add edges from r and the root node of the subtree to the new node. Now, the size of the currently constructed subtree is l' .

Repetition. We then repeat the above step, until all values in L_i are examined and the whole tree is constructed. We implement this method with a recursive algorithm, as shown in Algorithm 5.

Algorithm 5 Optimized version of FPRev-basic.

Require: Summation function SUM and number of summands n

Ensure: Summation tree T

function FPREVOPTIMIZED(SUM, n)

function BUILDSUBTREE(I)

$i \leftarrow \min(I)$

$T \leftarrow \emptyset$

if $|I| = 1$ **then** ▷ stop condition

return T

$L_i \leftarrow \emptyset$

for $j \in I - \{i\}$ **do** ▷ calculate $l^{i,j}$ on demand

 Construct $A^{i,j}$

$l^{i,j} \leftarrow n - \text{SUM}(A^{i,j})$

$L_i \leftarrow L_i \cup \{l^{i,j}\}$

$r \leftarrow i$ ▷ current root of the subtree

for $l \in L_i$ in ascending order **do**

$J_l \leftarrow \{j : j \in I - \{i\} \wedge l^{i,j} = l\}$

$T' \leftarrow \text{BUILDSUBTREE}(J_l)$

$T \leftarrow T \cup T'$

$T \leftarrow T \cup \{(r, r + n), (\text{GetRoot}(T'), r + n)\}$

$r \leftarrow r + n$

return T

return BUILDSUBTREE($\{0, 1, \dots, n - 1\}$)

4.1.2 Demonstration with example. Consider the summation tree in Figure 1. We construct the tree with Algorithm 5. First, the set of leaf nodes is $I = \{0, 1, \dots, 7\}$, where the smallest index is $i = 0$. Then, the set $L_i = \{l^{i,j} : j \in I - \{i\}\} = \{2, 4, 4, 6, 6, 8, 8\} = \{2, 4, 6, 8\}$ is calculated. Examining the smallest value in L_i , we have $l = 2$ and $J_l = \{j : j \in I - \{i\} \wedge l^{i,j} = l\} = \{1\}$. Therefore,

BUILDSUBTREE($\{1\}$) is called, reaching the stop condition. Then, the subtree with the 0th and 1st leaf nodes is constructed. The root of this subtree is denoted by r .

Next, examining the smallest value in the rest of L_i , we have $l = 4$ and $J_l = \{j : j \in I - \{i\} \wedge l^{i,j} = l\} = \{2, 3\}$. Therefore, BUILDSUBTREE($\{2, 3\}$) is called, where we have $I = \{2, 3\}$, $i = 2$, and $L_i = \{2\}$, and BUILDSUBTREE($\{3\}$) is called there. BUILDSUBTREE($\{2, 3\}$) returns the subtree with the 2nd and 3rd leaf nodes as its leaf nodes. We then take its root as the sibling node of r , and construct the parent node of this root and r . Then, the subtree with the 0th, 1st, 2nd, and 3rd leaf nodes is constructed. r is updated by the root of this subtree.

The next smallest value is $l = 6$. We have $J_l = \{4, 5\}$. Similarly, BUILDSUBTREE($\{4, 5\}$) is called, and it returns the subtree with the 4th and 5th leaf nodes. We merge its root with r , and construct the subtree with the 0th, 1st, 2nd, 3rd, 4th, and 5th leaf nodes. r is updated by the root of this subtree.

Finally, $l = 8$ and $J_l = \{6, 7\}$. BUILDSUBTREE($\{6, 7\}$) is called, and it returns the subtree with the 6th and 7th leaf nodes. We merge its root with r . Then the whole tree is constructed.

4.1.3 Time complexity. The time complexity of Algorithm 5 is $O(n^2t(n))$ and $\Omega(nt(n))$. The worst-case scenario occurs when adding n summands in the right-to-left order. In this case, BUILDSUBTREE will be invoked with all suffixes of $\{0, 1, \dots, n-1\}$, and $l^{i,j}$ for all $0 \leq i < j < n$ will be calculated. The worst-case time complexity is $\Theta(n^2t(n))$. In practice, this order is cache-unfriendly, and thus no library uses it.

The best-case scenario corresponds to the sequential summation, where the summation tree will be constructed in one pass, and only $l^{0,j}$ for all $0 < j < n$ will be calculated. The best-case time complexity is $\Theta(nt(n))$. In practice, many libraries use similar orders, because these orders are cache-friendly and efficient.

4.2 Extension

4.2.1 Multi-term fused summation. Matrix accelerators like NVIDIA Tensor Cores are specialized hardware components in recent GPUs. Matrix accelerators enable assembly instructions that take a matrix $A = (a_{ij})_{M \times K}$, a matrix $B = (b_{ij})_{K \times N}$, and a matrix $C = (c_{ij})_{M \times N}$ as input, and produce a matrix $D = (d_{ij})_{M \times N}$ such that $D = A \times B + C$. The data types of A and B are identical. The data types of C and D are also identical, and their precision is no lower than the precision of A and B .

The numerical behavior of matrix accelerators has not been disclosed. Specifically, the computation of $d_{ij} = c_{ij} + \sum_{k=0}^{K-1} a_{ik}b_{kj}$ is executed in an undocumented way. Prior work has proposed different guesses, such as chain of fused multiply-add operations (FMAs), pairwise summation, or multi-term fused summation [10, 14, 20, 26]. By conducting numerical experiments, we have reproduced the findings of [10, 20], which suggest that for low-precision input (specifically, when the precision of A and B is lower than float32), the computation of $d_{ij} = c_{ij} + \sum_{k=0}^{K-1} a_{ik}b_{kj}$ is executed in multi-term fused summation:

- The products are computed exactly, and the results are maintained in full precision without rounding after the multiplication.
- The summation of the $K + 1$ summands is performed in a fixed-point manner. Specifically, the significands are aligned to the largest exponent of the summands, and then truncated to 24+ bits (i.e., no less than the precision of float32). The number of bits and the truncation method depend on the GPU architecture.
- Then, the sum is converted to the floating-point number. The normalization method depends on the GPU architecture and the output data type of the instruction.

For higher-precision input, the computation is executed in a chain of standard FMAs. Our proposed methods, i.e., FPRev-basic and FPRev-optimized, can work for standard FMAs. However,

multi-term fused summation requires a new method, because it is executed in a non-standard, IEEE-754-incompliant way. Specifically, as shown in Algorithm 6, the $K + 1$ summands ($x_0 = c$, and $x_{i+1} = a_i b_i$ for $0 \leq i < K$) are summed in a fixed-point manner, thus making the result independent of the summation order. To represent this operation in the summation tree, we should use a node with $K + 1$ children instead of a node with two children. Therefore, the summation tree should be an $(K + 1)$ -way tree.

Algorithm 6 Multi-term fused summation

Require: Sequence $X = (x_0, x_1, \dots, x_K)$

Ensure: Floating-point sum of X

function FUSED SUM(X)

if there exists NaN or infinity in X **then**

return NaN or infinity according to IEEE-754

for all $0 \leq i \leq K$ **do**

$s_i \leftarrow$ Significant(x_i)

$e_i \leftarrow$ Exponent(x_i)

$E \leftarrow \max\{e_i\}$

for all $0 \leq i \leq K$ **do**

$z_i \leftarrow$ RShift($s_i, E - e_i$)

$S \leftarrow \sum_{i=0}^K z_i$

return fl($S \times 2^E$)

\triangleright can be parallel

$\triangleright 1 \leq |s_i| < 2$

$\triangleright s_i \times 2^{e_i} = x_i$

\triangleright can be parallel

\triangleright alignment and truncation

\triangleright fixed-point summation

\triangleright conversion

4.2.2 Constructing the multiway tree. To accommodate the multiway tree, we revisit our approach in Section 3. The first two stages keep working because we find that the key equation $l^{i,j} = n_{\text{leaves}}^{\text{LCA}(i,j)} = n - \text{SUM}(A^{i,j})$ remains valid in multi-term fused summation. Thus, the values of $l^{i,j}$ can be obtained in the same way, and we only need to redesign the tree construction algorithm in the third stage.

Then, we revisit the tree construction algorithm in Algorithm 5. In BUILD SUBTREE(I), we calculate $l^{i,j}$ for a fixed i and all $j \in I - \{i\}$, enumerate them in ascending order, and maintain r as the root of the largest constructed subtree containing the i -th leaf node. For some $l \in L_i = \{l^{i,j} : j \in I - \{i\}\}$ and $J_l = \{j : j \in I - \{i\} \wedge l^{i,j} = l\}$, the return value of BUILD SUBTREE(J_l) is the subtree with J_l as its leaf nodes. The root of this subtree must be the sibling node of r , so we can add a new node as their parent node and update r . However, this relation is not always true for the multiway tree.

In addition to being sibling node, the root of the subtree may also be the parent node of r in the multiway tree. For example, suppose a 5-way tree with leaf nodes $I = \{0, 1, 2, 3, 4\}$ as the children of the root. Then, when $r = 0$, $l = 5$, and $J_l = \{1, 2, 3, 4\}$, solving the subproblem for J_l should return a partial subtree with J_l as its leaves. The root node of the subtree is the parent node of r .

To distinguish the two cases, we observe the return value of BUILD SUBTREE(J_l), denoted by T' , and the complete subtree rooted at the root of T' , denoted by T_c . In the first case, the root of T' should be the sibling of r , and $T' = T_c$. In the second case, the root of T' should be the parent of r , and $T' \subset T_c$. Therefore, we can compare the size of T' (denoted by $n_{\text{leaves}}^{T'}$) with the size of T_c (denoted by $n_{\text{leaves}}^{T_c}$). We note that $n_{\text{leaves}}^{T'} = |J_l|$, and $n_{\text{leaves}}^{T_c} = \max\{l^{j,k} : j, k \in J_l\} = \max(L_{\min(J_l)})$. Therefore, if $\max(L_{\min(J_l)}) = |J_l|$, then the root of T' should be the sibling of r , so we should add a new node as their parent node and update r with the index of this new node. Otherwise, $\max(L_{\min(J_l)}) > |J_l|$, so the root of T' should be the parent of r , and thus we should add an edge from r to the root of T' , and update r with the root.

Through this modification, the multiway tree can be correctly constructed. We elaborate on the above process in Algorithm 7. We call it FPRev-advanced. FPRev-advanced has the same time complexity as Algorithm 5 (note that Algorithm 5 just corresponds to the case where $\max(L_{\min(J_i)}) = |J_i|$) and supports multi-term fused summation.

Algorithm 7 FPRev-advanced

Require: Summation function SUM and number of summands n

Ensure: Summation tree T

function FPREVADVANCED(SUM, n)

function BUILDSUBTREEADVANCED(I)

$i \leftarrow \min(I)$

$T \leftarrow \emptyset$

if $|I| = 1$ **then**

\triangleright stop condition

return T

$L_i \leftarrow \emptyset$

for $j \in I - \{i\}$ **do**

\triangleright calculate $l^{i,j}$ on demand

 Construct $A^{i,j}$

$l^{i,j} \leftarrow n - \text{SUM}(A^{i,j})$

$L_i \leftarrow L_i \cup \{l^{i,j}\}$

$r \leftarrow i$

\triangleright current root of the subtree

for $l \in L_i$ in ascending order **do**

$J_l \leftarrow \{j : j \in I - \{i\} \wedge l^{i,j} = l\}$

$(T', n_{\text{leaves}}^{T'}) \leftarrow \text{BUILDSUBTREEADVANCED}(J_l)$

$T \leftarrow T \cup T'$

if $|J_l| = n_{\text{leaves}}^{T'}$ **then**

$\triangleright T' = T_c$

$T \leftarrow T \cup \{(r, r + n), (\text{GetRoot}(T'), r + n)\}$

$r \leftarrow r + n$

else

$\triangleright T' \subset T_c$

$T \leftarrow T \cup \{(r, \text{GetRoot}(T'))\}$

$r \leftarrow \text{GetRoot}(T')$

return $(T, \max(L_i))$

$(T, n_{\text{leaves}}^{T'}) \leftarrow \text{BUILDSUBTREEADVANCED}(\{0, 1, \dots, n - 1\})$

return T

4.3 Time complexity and correctness

The time complexity of FPRev-advanced is $O(n^2t(n))$ and $\Omega(nt(n))$, following the same analysis in Section 4.1.3. The correctness of it is also guaranteed by design and can be proved following the same process in Section 3.4.

5 EVALUATION

5.1 Experiment design

In this section, we evaluate the efficiency of FPRev. Specifically, we aim to answer the following research questions:

- RQ1: How efficient is FPRev in revealing the order of summation for summation functions?
- RQ2: How efficient is FPRev in revealing the order of summation for different summation-based functions?

- RQ3: How efficient is FPRev on different CPUs and GPUs?

We implement the naive brute-force algorithm (Algorithm 3), FPRev-basic (Algorithm 4), and FPRev-advanced (Algorithm 7) with Python (version 3.11). We refer to these algorithms as “naive”, “basic”, and “advanced”.

For RQ1, we measure the run time (wall-clock time) of the three algorithms for summation functions in three libraries: NumPy (version 1.26) [12], PyTorch (version 2.3) [25], and JAX (version 0.4) [3].

For RQ2, we omit the naive algorithm, which has been proven to be too inefficient in the experiments for RQ1. We measure the run time of FPRev-basic and FPRev-advanced for the dot product, matrix–vector multiplication, and matrix–matrix multiplication functions in three libraries. The time complexity of these functions is $O(n)$, $O(n^2)$, and $O(n^3)$, respectively.

For RQ3, we measure the run time of FPRev-basic and FPRev-advanced for matrix multiplication functions in PyTorch² on different devices. Specifically, we conduct these experiments on three platforms (denoted by A, B, and C) with different CPUs and GPUs:

- A-CPU: Intel Xeon E5-2690 v4 (24 v-cores, 24 threads)
- A-GPU: NVIDIA V100 (80 SMs, 5120 CUDA cores)
- B-CPU: AMD EPYC 7V13 (24 v-cores, 24 threads)
- B-GPU: NVIDIA A100 (108 SMs, 6912 CUDA cores)
- C-CPU: Intel Xeon Platinum 8480C (96 v-cores, 96 threads)
- C-GPU: NVIDIA H100 (132 SMs, 16896 CUDA cores)

5.2 RQ1: How efficient is FPRev in revealing the order of summation for summation functions?

The experiments for RQ1 are conducted on A-CPU using the float32 data type. We start with the number of summands $n = 4$, and increase n until the run time exceeds one second. The results are shown in Figure 2. Each experiment represents a specific combination of revelation algorithm, library, and number of summands n . Each experiment is carried out 10 times, and the arithmetic mean of the 10 results is reported in Figure 2.

The orange curves show that the run time of the naive algorithm grows exponentially as n grows. The results substantiate the $O(4^n/n^{3/2} \cdot t(n))$ time complexity of the naive algorithm. The green and blue lines show that the run time of FPRev-basic and that of FPRev-advanced grows polynomially. The results also show that the run time of FPRev-basic is longer than that of FPRev-advanced, and grows faster as n increases. This is because the time complexity of FPRev-basic is $\Theta(n^2t(n))$, while the time complexity of FPRev-advanced is $\Omega(nt(n))$ and $O(n^2t(n))$.

These trends suggest that the scalability of FPRev-basic is much better than that of the naive algorithm, and the scalability of FPRev-advanced is even better. For example, if $n = 16$, the naive algorithm can take more than 24 hours to produce an output, but FPRev-basic and FPRev-advanced only take less than 0.01 seconds. If $n = 8192$, FPRev-basic will take more than 100 seconds to produce an output, but FPRev-advanced only takes about one second.

5.3 RQ2: How efficient is FPRev in revealing the order of summation for different summation-based functions?

The experiments for RQ2 are conducted on A-CPU using the float32 data type. Similarly, we start with $n = 4$, and increase n until the run time exceeds one second. Each experiment is carried out 10 times, and the arithmetic mean of the 10 results is reported in Table 3. (The results for the

²NumPy does not support GPU. The backend library of both PyTorch and JAX is the same (i.e., cuBLAS) on NVIDIA GPUs.

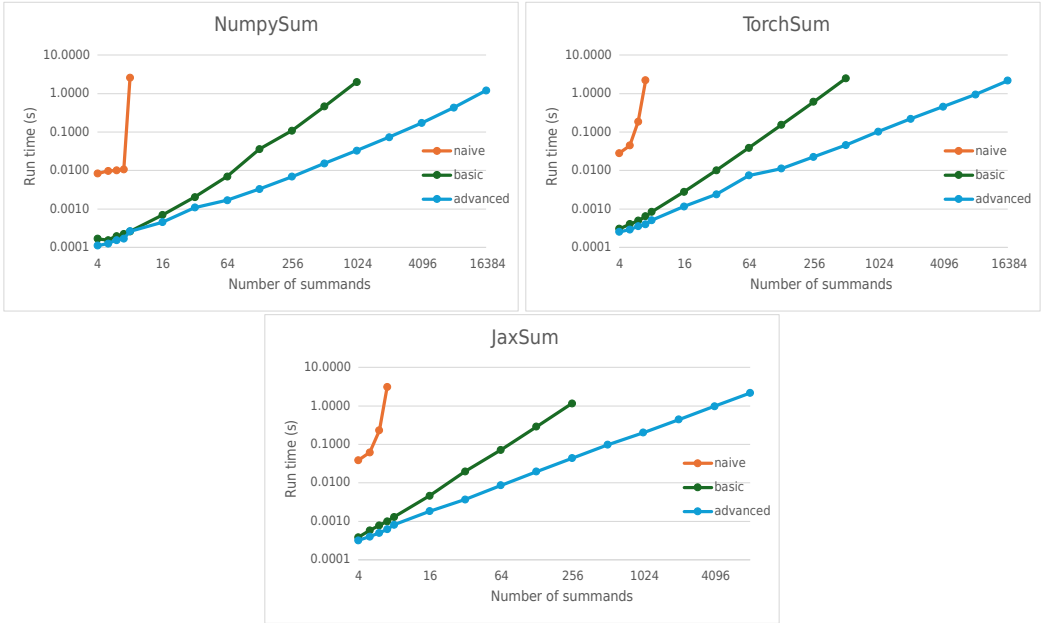


Fig. 2. Run time for revealing the order of summation in NumPy, PyTorch, and JAX with the naive, basic, and advanced methods. The vertical axis is run time in seconds. The horizontal axis is the number of summands n .

matrix-matrix multiplication functions are omitted because of space limit, and will be available online.) Empty cells represent that the run time significantly exceeds one second.

The results show that the run time of FPREv-basic is longer than the run time of FPREv-advanced, and grows faster as n increases. In addition, as the time complexity of the workload increases, the growth speed of the runtime with regard to n accelerates. Therefore, the speedup of FPREv-advanced versus FPREv-basic is more pronounced as the workload is more complex.

For example, for the dot product functions in the three libraries, the geometric mean of the speedups of FPREv-advanced versus FPREv-basic is $2.62\times$ for $n = 16$, and $15.38\times$ for $n = 128$. For the matrix-vector multiplication functions, the geometric mean of speedups is $3.42\times$ for $n = 16$, and $35.67\times$ for $n = 128$. For the matrix-matrix multiplication functions, the geometric mean of speedups is $4.12\times$ for $n = 16$, and $53.70\times$ for $n = 128$.

5.4 RQ3: How efficient is FPREv on different CPUs and GPUs?

The experiments for RQ3 are conducted on A-CPU, A-GPU, B-CPU, B-GPU, C-CPU, and C-GPU using the float32 data type. Similarly, we start with $n = 4$, and increase n until the run time exceeds one second. Each experiment is carried out 10 times, and the arithmetic mean of the 10 results is reported in Table 4.

The results show consistent improvements in the run time of FPREv-advanced versus FPREv-basic. Therefore, FPREv-advanced is more efficient than FPREv-basic on different CPUs and GPUs.

6 REVEALED SUMMATION ORDERS

In this section, we aim to answer the following research questions by showcasing some orders of summation revealed by FPREv.

- RQ4: Are different orders of summation observed across different libraries?

Table 3. Run time in seconds for revealing the order of operations in the dot product and matrix-vector multiplication functions in NumPy, PyTorch and JAX using FPRRev-basic and FPRRev-advanced. Empty cells represent timeout.

n	NumpyDot		TorchDot		jaxDot		NumpyGEMV		TorchGEMV		jaxGEMV	
	basic	advanced	basic	advanced	basic	advanced	basic	advanced	basic	advanced	basic	advanced
4	0.00014	0.00012	0.00035	0.00030	0.00034	0.00024	0.00015	0.00013	0.00043	0.00039	0.00122	0.00067
8	0.00026	0.00020	0.00088	0.00065	0.00104	0.00044	0.00029	0.00023	0.00117	0.00069	0.00555	0.00149
16	0.00068	0.00037	0.00290	0.00138	0.00368	0.00080	0.00077	0.00043	0.00406	0.00135	0.02245	0.00303
32	0.00224	0.00100	0.01079	0.00304	0.01523	0.00154	0.00239	0.00087	0.01556	0.00243	0.08805	0.00610
64	0.00763	0.00202	0.04254	0.00662	0.05791	0.00307	0.00873	0.00176	0.06280	0.00459	0.36301	0.01233
128	0.03630	0.00401	0.15306	0.01450	0.22875	0.00601	0.16700	0.00750	0.34565	0.01004	1.53696	0.02595
256	0.10465	0.00807	0.61788	0.02977	0.92213	0.01210	0.71664	0.02215	1.70408	0.02072	0.05123	0.05123
512	0.42698	0.01546	2.51626	0.06142	3.78066	0.02445	5.02031	0.05548	0.05648	0.05648	0.11312	0.11312
1024	1.84475	0.03224		0.12324		0.04925		0.23766		0.27945	0.32024	0.32024
2048		0.06431		0.25404		0.10267		0.67724		0.31079	1.46030	1.46030
4096		0.13521		0.52728		0.21915		19.27085		4.18472		
8192		0.28186		1.38307		0.49702						
16384		0.69205				1.24560						
32768		1.87398										

Table 4. Run time in seconds for revealing the order of operations in the matrix-matrix multiplication function in PyTorch with FPRRev-basic and FPRRev-advanced on different devices. Empty cells represent timeout.

n	A.CPU		A.GPU		B.CPU		B.GPU		C.CPU		C.GPU	
	basic	advanced	basic	advanced	basic	advanced	basic	advanced	basic	advanced	basic	advanced
4	0.00045	0.00040	0.00114	0.00078	0.00022	0.00019	0.00065	0.00046	0.00016	0.00017	0.00065	0.00041
8	0.00125	0.00079	0.00431	0.00209	0.00062	0.00036	0.00223	0.00121	0.00044	0.00031	0.00164	0.00098
16	0.00466	0.00159	0.01638	0.00542	0.00212	0.00071	0.00895	0.00195	0.00172	0.00060	0.00636	0.00228
32	0.01810	0.00343	0.06556	0.00643	0.01461	0.00179	0.03238	0.00584	0.00679	0.00124	0.02240	0.00700
64	0.11473	0.00810	0.25203	0.02205	0.05977	0.00357	0.12834	0.01196	0.27901	0.00867	0.08552	0.01500
128	0.73907	0.01467	0.99224	0.04196	0.28069	0.00772	0.52889	0.02241	0.90428	0.01775	0.32772	0.02881
256	3.51068	0.03431	4.11688	0.08044	1.84963	0.02857	2.21939	0.05613	4.96277	0.17905	1.50927	0.05948
512		0.35281		0.18761		0.19230		0.10890		0.14732		0.12560
1024		3.59237		0.63623		2.52039		0.39472		1.92971		0.31785
2048				5.85436				2.21231				0.93580
4096												6.93602

- RQ5: Are different orders of summation observed on different devices?

6.1 RQ4: Are different orders of summation observed across different libraries?

We run FPRev-advanced for the summation functions in NumPy, PyTorch, and JAX on A-CPU using the float32 data type. We examine the revealed summation trees for n from 4 to 2048. The results show that on NumPy uses multi-lane strided summation and reduce them with pairwise summation. PyTorch uses multi-level strided summation and reduce them with sequential summation. JAX uses multi-lane strided summation and reduce them with pairwise summation, but the number of lanes and the reduction order are different from NumPy. For example, Figure 3 shows the summation trees of the libraries for $n = 64$.

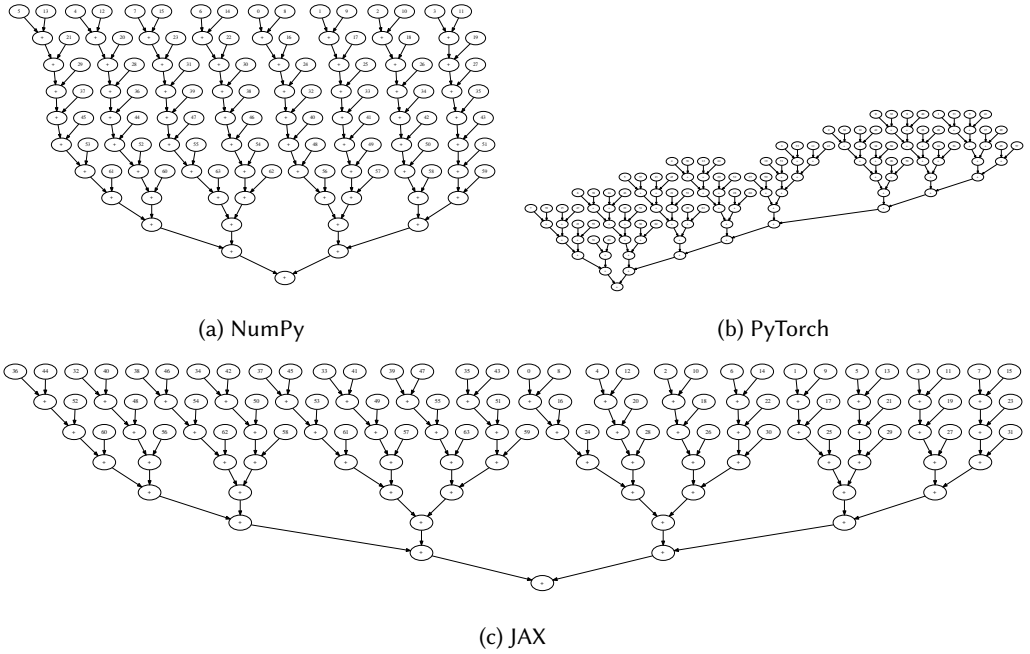


Fig. 3. The summation trees of different libraries for summation of 64 numbers.

6.2 RQ5: Are different orders of summation observed on different devices?

We run FPRev-advanced for the matrix multiplication function in PyTorch on A-GPU, B-GPU, and C-GPU, using the float16 data type to enable Tensor Core computation. We examine the revealed summation trees for n from 16 to 2048. The results show that on A-GPU (NVIDIA V100), the summation tree is a 5-way tree; on B-GPU (NVIDIA A100), the summation tree is a 9-way tree; on C-GPU (NVIDIA H100), the summation tree is a 17-way tree. For example, Figure 4 shows the summation tree for $n = 32$ on these devices.

Our results corroborate the conclusion in [10, 20], which states that the Tensor Cores on NVIDIA Volta, Ampere, and Hopper architectures use (4+1), (8+1), and (16+1)-term fused summation respectively.

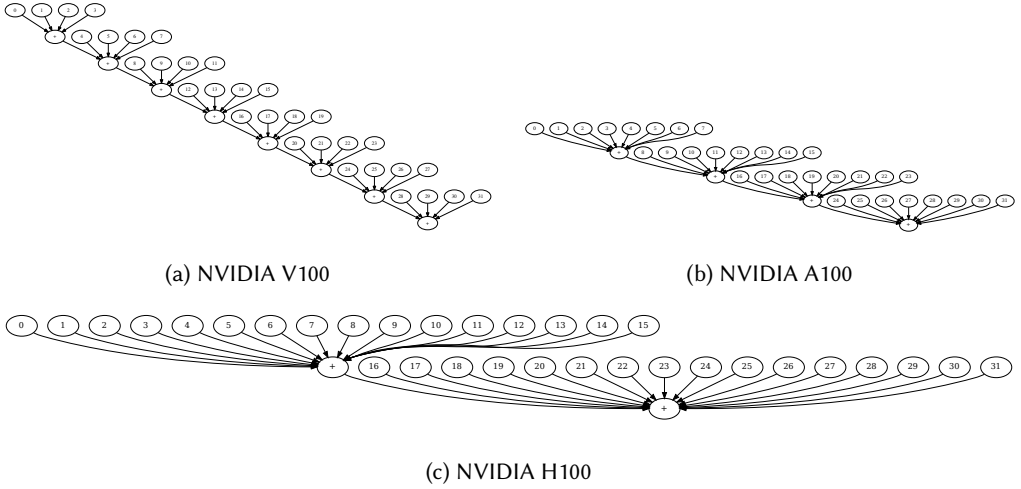


Fig. 4. The summation trees for $32 \times 32 \times 32$ matrix multiplication on Tensor Cores

7 DISCUSSION

7.1 Threats to validity

7.1.1 Internal. The precision of the floating-point data type can limit the validity of our tool. For float32, whose precision is 24 bits, the maximum number of summands (n) that our tool supports is $2^{24} + 1 = 16777217$. For larger numbers, the sum of $n - 2$ ones cannot be represented precisely by float32, so the sum of masked all-one arrays may be incorrect. This problem could be solved by replacing the multiple ones corresponding to a constructed subtree in the masked all-one arrays with a single one and multiple zeros. This solution does not affect efficiency.

For low-precision data types, there is an additional issue on the floating-point swamping because $M \ll n$ may not hold. For example, the maximum exponent of float16 is 15. If $M = 2^{15}$ and $\mu = 256$, $\pm M + \mu \neq \pm M$. To solve this problem, we can replace the ones of the masked all-one arrays by smaller numbers (e.g., 2^{-24}), and scale the sum back to an integer between 0 and $n - 2$ when calculating $l^{i,j}$. This solution does not affect efficiency, either.

7.1.2 External. If the tested function has functional defects, our tool may not yield a correct result. Nonetheless, we can still identify some causes of non-reproducibility from the output of our tool. For example, our tool is effective in detecting the decrease in precision. If there is a conversion from float64 to float32 during summation, our tool will detect overflows, indicating the presence of the conversion.

For non-reproducibility caused by randomization, it is easy to tell whether the function is randomized or deterministic by repeated testing. For non-reproducibility caused by switching instruction fusion, our tool can still yield the correct result, as it supports fused multiply-add instructions and fused multi-term addition instructions.

7.2 Extensibility

The scope of our tool has been detailed in Section 2. In addition, our tool has been extended to support Algorithm 6 (the fused multi-term summation algorithm). As a result, our tool supports summation-based functions in most popular numerical libraries. Our tool also works for collective communication primitives if their order of summation is predetermined. To further extend our tool

for other functions based on special summation algorithms, the algorithms must have the property $n_{\text{leaves}}^{\text{LCA}(i,j)} = n - \text{SUM}(A^{i,j})$. Thus, our methods can be abstracted as a template to reveal the order of summation.

8 RELATED WORK

8.1 Debugging of non-reproducibility

The debugging of floating-point non-reproducibility is a significant challenge. Diverse factors, including hardware, compilers, algorithms, etc., can influence reproducibility [1]. They may introduce mathematical transformations that are semantically equivalent in real numbers but differ in floating-point arithmetic. To identify the root causes of numerical non-reproducibility, we need to figure out how the calculation is transformed. Previous work has used differential testing to identify the non-reproducible parts of a program [11, 19, 23]. However, this is insufficient to identify the root cause of non-reproducibility; people still need to scrutinize the trace or the code manually.

8.2 Floating-point summation

Summation functions underpin high-level operations in numerical computing, such as dot products, vector norms, convolutions, matrix multiplications, and stencils. Many numerical computing applications frequently invoke these functions, so ensuring their numerical reproducibility is crucial for the overall reproducibility of the applications.

Previous work [27, 30] has identified the primary cause of non-reproducibility of the summation-based functions: varying orders of summation. However, the previous work cannot provide detailed information about how the order of summation is transformed, making it difficult to examine and reproduce existing functions.

There are special summation algorithms that are not based on pure floating-point addition, such as Kahan’s summation algorithm [18]. Notably, order-independent summation algorithms have been proposed [6, 8, 9]. These algorithms ensure that the result of summation remains consistent regardless of the order. However, they are inefficient and are therefore not widely used.

8.3 Revelation of numerical behaviors

Previous work has employed testing-based approaches to detect numerical errors for software [5, 31] or analyze numerical behaviors for hardware [10, 14, 20]. The authors run numerical experiments with well-designed input, and analyze the numerical behaviors of the tested software or hardware based on the output. However, to our knowledge, we are the first to employ testing-based approaches to reveal the order of floating-point summation.

9 CONCLUSION

In this paper, we introduce FPRev, a testing-based tool for revealing the order of floating-point summation. We demonstrate its efficiency through experiments that cover various workloads and devices, and show the different orders of summation for common numerical libraries. Our source code and test cases are available online, encouraging further investigation and improvement by the research community.

REFERENCES

- [1] Andrea Arteaga, Oliver Fuhrer, and Torsten Hoefler. Designing Bit-Reproducible Portable High-Performance Applications. In *IEEE International Parallel and Distributed Processing Symposium (IPDPS)*, pages 1235–1244, 2014. doi:10.1109/IPDPS.2014.127.

- [2] David H Bailey, Jonathan M Borwein, and Victoria Stodden. Facilitating reproducibility in scientific computing: Principles and practice. In *Reproducibility: Principles, Problems, Practices, and Prospects*, pages 205–231. Wiley Online Library, 2016. Publisher: Wiley Online Library.
- [3] James Bradbury, Roy Frostig, Peter Hawkins, Matthew James Johnson, Chris Leary, Dougal Maclaurin, George Necula, Adam Paszke, Jake VanderPlas, Skye Wanderman-Milne, and Qiao Zhang. JAX: composable transformations of Python+NumPy programs, 2018. URL: <http://github.com/google/jax>.
- [4] Boyuan Chen, Mingzhi Wen, Yong Shi, Dayi Lin, Gopi Krishnan Rajbahadur, and Zhen Ming Jiang. Towards Training Reproducible Deep Learning Models. In *International Conference on Software Engineering (ICSE)*, pages 2202–2214, 2022. doi: 10.1145/3510003.3510163.
- [5] Wei-Fan Chiang, Ganesh Gopalakrishnan, Zvonimir Rakamaric, and Alexey Solovyev. Efficient search for inputs causing high floating-point errors. In *ACM Symposium on Principles and Practice of Parallel Programming (PPoPP)*, pages 43–52, 2014. doi: 10.1145/2555243.2555265.
- [6] Sylvain Collange, David Defour, Stef Graillat, and Roman Iakymchuk. Numerical Reproducibility for the Parallel Reduction on Multi- and Many-Core Architectures. *Parallel Computing*, 49:83–97, 2015. doi: 10.1016/j.parco.2015.09.001.
- [7] OpenBLAS Contributors. Openblas: An optimized blas library. URL: <https://www.openblas.net/>.
- [8] James Demmel and Hong Diep Nguyen. Fast Reproducible Floating-Point Summation. In *IEEE Symposium on Computer Arithmetic (ARITH)*, pages 163–172, 2013. doi: 10.1109/ARITH.2013.9.
- [9] James Demmel and Hong Diep Nguyen. Parallel Reproducible Summation. *IEEE Transactions on Computers*, 64(7):2060–2070, 2015. doi: 10.1109/TC.2014.2345391.
- [10] Massimiliano Fasi, Nicholas J. Higham, Mantas Mikaitis, and Srihara Pranesh. Numerical behavior of NVIDIA tensor cores. *PeerJ Computer Science*, 7:e330, 2021. doi: 10.7717/peerj-cs.330.
- [11] Hui Guo, Ignacio Laguna, and Cindy Rubio-González. pLiner: isolating lines of floating-point code for compiler-induced variability. In *International Conference for High Performance Computing, Networking, Storage and Analysis (SC)*, page 49, 2020. doi: 10.1109/SC41405.2020.00053.
- [12] Charles R. Harris, K. Jarrod Millman, Stéfan van der Walt, Ralf Gommers, Pauli Virtanen, David Cournapeau, Eric Wieser, Julian Taylor, Sebastian Berg, Nathaniel J. Smith, Robert Kern, Matti Picus, Stephan Hoyer, Marten H. van Kerkwijk, Matthew Brett, Allan Haldane, Jaime Fernández del Río, Mark Wiebe, Pearu Peterson, Pierre Gérard-Marchant, Kevin Sheppard, Tyler Reddy, Warren Weckesser, Hameer Abbasi, Christoph Gohlke, and Travis E. Oliphant. Array programming with NumPy. *Nature*, 585:357–362, 2020. URL: <https://doi.org/10.1038/s41586-020-2649-2>, doi: 10.1038/S41586-020-2649-2.
- [13] Yun He and Chris H. Q. Ding. Using Accurate Arithmetics to Improve Numerical Reproducibility and Stability in Parallel Applications. *The Journal of Supercomputing*, 18(3):259–277, 2001. doi: 10.1023/A:1008153532043.
- [14] Brian J. Hickmann and Dennis Bradford. Experimental Analysis of Matrix Multiplication Functional Units. In *IEEE Symposium on Computer Arithmetic (ARITH)*, pages 116–119, 2019. doi: 10.1109/ARITH.2019.00031.
- [15] Nicholas J. Higham. The Accuracy of Floating Point Summation. *SIAM Journal on Scientific Computing*, 14(4):783–799, 1993. doi: 10.1137/0914050.
- [16] IEEE. *IEEE Standard for Floating-Point Arithmetic*, 2019. doi: 10.1109/IEEESTD.2019.8766229.
- [17] Intel Corporation. *Intel Math Kernel Library*. URL: <https://www.intel.com/content/www/us/en/developer/tools/oneapi/onemkl.html>.
- [18] William Kahan. Further remarks on reducing truncation errors. *Communications of the ACM*, 8(1):40, 1965. doi: 10.1145/363707.363723.
- [19] Ignacio Laguna. Varity: Quantifying Floating-Point Variations in HPC Systems Through Randomized Testing. In *IEEE International Parallel and Distributed Processing Symposium (IPDPS)*, pages 622–633, 2020. doi: 10.1109/IPDPS47924.2020.00070.
- [20] Xinyi Li, Ang Li, Bo Fang, Katarzyna Swirydowicz, Ignacio Laguna, and Ganesh Gopalakrishnan. FTTN: Feature-Targeted Testing for Numerical Properties of NVIDIA & AMD Matrix Accelerators, 2024. arXiv: 2403.00232. URL: <https://doi.org/10.48550/arXiv.2403.00232>, doi: 10.48550/ARXIV.2403.00232.
- [21] Chao Liu, Cuiyun Gao, Xin Xia, David Lo, John C. Grundy, and Xiaohu Yang. On the Reproducibility and Replicability of Deep Learning in Software Engineering. *ACM Transactions on Software Engineering and Methodology*, 31(1):15:1–15:46, 2022. doi: 10.1145/3477535.
- [22] Stefano Markidis, Steven Wei Der Chien, Erwin Laure, Ivy Bo Peng, and Jeffrey S. Vetter. NVIDIA Tensor Core Programmability, Performance & Precision. In *IEEE International Parallel and Distributed Processing Symposium (IPDPS) Workshops*, pages 522–531. IEEE Computer Society, 2018. doi: 10.1109/IPDPSW.2018.00091.
- [23] Dolores Miao, Ignacio Laguna, and Cindy Rubio-González. Expression Isolation of Compiler-Induced Numerical Inconsistencies in Heterogeneous Code. In *ISC High Performance*, pages 381–401, 2023. URL: https://doi.org/10.1007/978-3-031-32041-5_20, doi: 10.1007/978-3-031-32041-5_20.

- [24] NVIDIA Corporation. *cuBLAS: Basic Linear Algebra on NVIDIA GPUs*. URL: <https://developer.nvidia.com/cublas/>.
- [25] Adam Paszke, Sam Gross, Francisco Massa, Adam Lerer, James Bradbury, Gregory Chanan, Trevor Killeen, Zeming Lin, Natalia Gimelshein, Luca Antiga, Alban Desmaison, Andreas Köpf, Edward Z. Yang, Zachary DeVito, Martin Raison, Alykhan Tejani, Sasank Chilamkurthy, Benoit Steiner, Lu Fang, Junjie Bai, and Soumith Chintala. PyTorch: An Imperative Style, High-Performance Deep Learning Library. In *Conference on Neural Information Processing Systems (NeurIPS)*, pages 8024–8035, 2019. URL: <https://proceedings.neurips.cc/paper/2019/hash/bdbca288fee7f92f2bfa9f7012727740-Abstract.html>.
- [26] Md Aamir Raihan, Negar Goli, and Tor M. Aamodt. Modeling Deep Learning Accelerator Enabled GPUs. In *IEEE International Symposium on Performance Analysis of Systems and Software (ISPASS)*, pages 79–92, 2019. doi: 10.1109/ISPASS.2019.00016.
- [27] Robert W. Robey, Jonathan M. Robey, and Rob Aulwes. In search of numerical consistency in parallel programming. *Parallel Computing*, 37(4-5):217–229, 2011. URL: <https://doi.org/10.1016/j.parco.2011.02.009>, doi: 10.1016/J.PARCO.2011.02.009.
- [28] Robert Endre Tarjan and Jan van Leeuwen. Worst-case Analysis of Set Union Algorithms. *Journal of the ACM*, 31(2):245–281, 1984. doi: 10.1145/62.2160.
- [29] Michela Taufer, Omar Padron, Philip Saponaro, and Sandeep Patel. Improving numerical reproducibility and stability in large-scale numerical simulations on GPUs. In *IEEE International Parallel and Distributed Processing Symposium (IPDPS)*, pages 1–9, 2010. doi: 10.1109/IPDPS.2010.5470481.
- [30] Oreste Villa, Daniel Chavarria-Miranda, Vidhya Gurumoorthi, Andrés Márquez, and Sriram Krishnamoorthy. Effects of floating-point non-associativity on numerical computations on massively multithreaded systems. In *Cray User Group Meeting (CUG)*, volume 3, 2009.
- [31] Daming Zou, Ran Wang, Yingfei Xiong, Lu Zhang, Zhendong Su, and Hong Mei. A Genetic Algorithm for Detecting Significant Floating-Point Inaccuracies. In *International Conference on Software Engineering (ICSE)*, pages 529–539, 2015. doi: 10.1109/ICSE.2015.70.